6

Experimental observation of GW emission in compact binaries

In this chapter we discuss the experimental evidence for the existence of GWs, which has been first obtained from the Hulse–Taylor binary pulsar, PSR B1913+16, and which is by now further confirmed by observations in other relativistic binary systems. As we will see, these binary pulsars turn out to be remarkable laboratories, that allow us to verify with high precision various predictions of general relativity.

Hulse and Taylor were awarded the Nobel Prize in 1993, "for the discovery of a new type of pulsar, a discovery that has opened up new possibilities for the study of gravitation", including the demonstration of the emission of gravitational radiation, obtained by Taylor and coworkers in the late 1970s and early 1980s.

6.1 The Hulse–Taylor binary pulsar

The pulsar PSR B1913+16,[1] or Hulse–Taylor binary pulsar, was first detected in July 1974, during a systematic survey for new pulsars carried out at the Arecibo Observatory in Puerto Rico. It was detected as a pulsar with a period $P \simeq 59$ ms. The period however had apparent changes up to $\sim 80\,\mu$s from day to day. For comparison, the largest secular changes in period, for pulsars, were known to be of order $10\,\mu$s *per year*. It soon became clear that the observed changes in period were due to the Doppler shift resulting from the orbital motion of the pulsar around a companion, and by September 1974 an accurate velocity curve had been obtained (Hulse and Taylor, 1975).

Nowadays, after about 30 years of observation, this binary system is known extraordinarily well. To have an idea of the impressive precision, we report in Table 6.1 the measured values of the orbital parameters, with their experimental error. Observe in particular that the orbital period P_b of the binary is less than 8 hours. This means that the orbital velocity is of order $v \sim 10^{-3}c$. Thus, this system is quite relativistic.

The geometry of the system is illustrated in Fig. 6.1. The relative coordinate between the pulsar and its companion, $\mathbf{r} = \mathbf{r}_p - \mathbf{r}_c$, describes an ellipse of eccentricity e, whose normal makes an angle ι with respect to the line of sight, which we take to be the z axis. The orbit intersects

[1] Pulsars are identified by the prefix PSR, followed by their equatorial coordinates (α, δ). The right ascension α is measured in hours and minutes, $0 \leqslant \alpha < 24$ hr, while the declination $\delta \in [-90°, +90°]$ (see e.g. Binney and Merrifield (1998) for definitions). In PSR B1913+16, 1913 means that the right ascension is $\alpha = 19$h13m and the declination is $\delta = +16°$. If more precision is required, one uses, e.g. PSR B1913+167, which means that the declination is $\delta = +(16.7)°$. If one use 1950 coordinates, the prefix B is added before the right ascension, while in 2000 coordinates the prefix J is used. The convention is that all pulsars published after 1993 retain only their J designation, while for the others both names can be used. The Hulse–Taylor pulsar can then be denoted as PSR B1913+16 as well as PSR J1915+1606. If various pulsars are very close to each other, they are designated appending a letter at the end; e.g. in the double pulsar system PSR J0737−3039, the two pulsars are identifies as PSR J0737−3039A and PSR J0737−3039B. In the globular cluster 47 Tucanae there are 20 pulsars so close together, that they are denoted by PSR J0021−72C, PSR J0021−72D, etc. (see the ATNF pulsar catalogue).

Table 6.1 The orbital parameters of PSR B1913+16. a_p is the semimajor axis of the pulsar orbit and ι the inclination of the orbit with respect to the line of sight; e is the eccentricity; T_0 is a time of passage at periastron (in Mean Julian Day), used as a reference epoch; P_b is the binary orbital period, at the reference epoch; ω_0 is the angle made by the periastron, measured from the ascending node, at the reference epoch; $\langle\dot\omega\rangle$ is the advance rate of the periastron, averaged over one orbital period; γ is the Einstein parameter (see below); $\dot P_b$ is the time derivative of the orbital period. The number in parentheses is the error on the last digit. From Weisberg and Taylor (2004).

Parameter	Value
$(1/c)a_p \sin\iota$ (s)	2.3417725(8)
e	0.6171338(4)
T_0 (MJD)	52144.90097844(5)
P_b (days)	0.322997448930(4)
ω_0 (deg)	292.54487(8)
$\langle\dot\omega\rangle$ (deg/yr)	4.226595(5)
γ (s)	0.0042919(8)
$\dot P_b$	$-2.4184(9) \times 10^{-12}$

the (x, y) plane in two points, or "nodes". The line connecting these two points is called the line of nodes. The node at which the coordinate r enters from below the upper hemisphere is called the ascending node. The angular position of the periastron, measured from the ascending node, is denoted by ω.[2]

Another very interesting value from Table 6.1 is that of the advance of the periastron, $\dot\omega$, which is more than 4 degrees per year. By comparison, the advance of the periastron of Mercury, which is one of the classical tests of general relativity, is 43 arcsec per century. This shows how general-relativistic effects are important in this binary system.

In the next section we will discuss in detail how, from the analysis of the time of arrivals of the pulses, one can extract very rich information and perform accurate tests of general relativity, including the verification of the emission of gravitational radiation. Here we summarize the main results that will be derived below.

From the measured value of $\langle\dot\omega\rangle$ and of the Einstein parameter γ we can obtain the masses of the pulsar, m_p, and of its companion, m_c. The result is (Weisberg and Taylor 2004)

$$m_p = 1.4414(2) M_\odot\,, \qquad m_c = 1.3867(2) M_\odot\,. \tag{6.1}$$

Again, the precision of these determinations is quite remarkable. (When inserting the numerical values, it is useful to recall that the quantity $GM_\odot$ is known to much better precision than G and $M_\odot$ separately.) The semimajor axis a is then determined by the usual Keplerian expres-

[2] In this chapter we will follow the notation which is commonly used in the pulsar literature. In particular the letter ω, that in the rest of the book denotes an angular velocity, here is the periastron angle; we will also use P to denote the spinning period of the pulsar, $\nu = 1/P$ its frequency, and P_b the orbital period of the binary system.

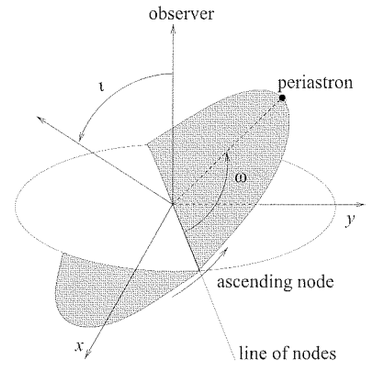

Fig. 6.1 The geometry of the orbit. The plane of the orbit is in gray.

sion

$$a = [G(m_p + m_c)]^{1/3} \left(\frac{P_b}{2\pi}\right)^{2/3} , \tag{6.2}$$

which gives $a \simeq 2.2 \times 10^9$ m; for comparison, the solar radius is $R_\odot \simeq 7 \times 10^8$ m, so the semimajor axis of the orbit is only about $3R_\odot$. This compactness of the orbit, together with the fact that no eclipse is seen, implies that the companion must be a compact star, i.e. a NS or a BH. This is very important for the following analysis, since it means that the dynamics of the binary system can be studied treating the two stars as pointlike bodies, ignoring for instance tidal effects. Thus, we have a very clean system. Actually, the value of m_c found above is the typical value expected for a NS, so it is believed that the companion is a NS.

The semimajor axis of the pulsar orbit, a_p, and of its companion, a_c, can now be obtained from

$$a_p = a \frac{m_c}{m_p + m_c} , \qquad a_c = a \frac{m_p}{m_p + m_c} . \tag{6.3}$$

Having a_p, from the measured value of $a_p \sin\iota$ given in Table 6.1 we also get the inclination angle, $\sin\iota \simeq 0.72$. Finally, having the masses of the two stars and the eccentricity, general relativity predicts that the orbital period decreases because of GW emission. We first computed this effect within linearized theory using an energy balance argument, and we found (eq. (4.79), with the present change in notation $T \to P_b$)

$$\dot{P}_b = -\frac{192\pi G^{5/3}}{5c^5} m_p m_c (m_p + m_c)^{-1/3} \left(\frac{P_b}{2\pi}\right)^{-5/3} \times \frac{1}{(1-e^2)^{7/2}} \left(1 + \frac{73}{24}e^2 + \frac{37}{96}e^4\right) . \tag{6.4}$$

However, as we discussed in Section 5.3.5, this result can also be obtained *directly* from the post-Newtonian equations of motion of the binary system, using the formalism discussed in Sections 5.2–5.4, without invoking the energy balance argument. Furthermore, we have seen in Section 5.5 that this result applies even in the presence of strong gravitational fields, which is indeed the case for neutron stars.

We can therefore compare the value predicted by general relativity, and due to the emission of GW radiation, with the observed value given in Table 6.1. After including a Doppler correction due to the relative velocity between us and the pulsar induced by the differential rotation of the Galaxy, one finds that the ratio between the experimental value $(\dot{P}_b)_{\rm exp}$ and the value $(\dot{P}_b)_{\rm GR}$ predicted by general relativity is

$$(\dot{P}_b)_{\rm corrected}/(\dot{P}_b)_{\rm GR} = 1.0013(21) . \tag{6.5}$$

This provides a wonderful confirmation of general relativity, as well as of the existence of GWs. In the next section we will discuss how these results are extracted from the timing residuals of the pulsar.

Beside its obvious intrinsic interest, the techniques used to correct the pulsar signal for various effects, due both to the motion of the Earth and to intrinsic changes in the source, will also be very important when searching for periodic GWs emitted from pulsars, as we will discuss in Section 7.6, so we will examine the timing formula in some detail.

6.2 The pulsar timing formula

6.2.1 Pulsars as stable clocks

Neutron stars are rapidly spinning, with rotational periods as small as 1.5 ms. This is a consequence of the conservation of angular momentum during the collapse, since ωr^2 stays constant while r decreases from the typical stellar size of the original star core down to a radius of just 10 km. It is thought that the supernova collapse can spin them up to maybe 10 ms. Neutron stars in binary system can be further spin up by accretion of mass from the companion. Similarly, because of the conservation of the magnetic flux during the collapse, neutron stars have huge magnetic fields, as large as 10^{12} gauss and higher (however, the accretion process in binaries tends to decrease the field somewhat). The magnetic field is in general misaligned with the rotation axis, so it has the structure of a rotating dipole, as in Fig. 6.2. If ρ denotes the distance from the rotation axis in cylindrical coordinates, there is a critical distance $\rho_c = c/\Omega$ (where Ω is the angular velocity of the pulsar) such that the magnetic field lines that reach a distance $\rho > \rho_c$ are open and escape to infinity, while those contained within ρ_c are closed. Observe that ρ_c is the maximum distance at which an object can corotate with the pulsar, without exceeding the speed of light.

Inside this cylinder of radius ρ_c there is a "magnetosphere" made of an ionized high-energy plasma, mostly corotating with the neutron star. High-energy particles in the magnetosphere are constrained to move along the open field lines over the magnetic poles, and emit radiation, most easily observed in the radio waves, narrowly focused in the direction of the magnetic poles, so each beam sweeps a circle in the sky. An observer that happens to be along one point of this circle therefore receives a short radio pulse when the beam of radiation sweeps along her line of sight, much like from a lighthouse, and the periodicity of the pulse is equal to the rotational period of the neutron star. Given the huge value of the moment of inertia of a NS, of order $10^{45}\,{\rm gr\,cm^2}$, we can understand that the pulse period can be extremely stable.

Actually, if one observes single pulses from a given pulsar, one finds that each pulse has its own profile, which can very dramatically, reflecting fluctuations in the radiation mechanism related to the complex dynamics of the magnetosphere. However, if one performs a coherent addition of many pulses, it usually emerges a single profile, which is a fingerprint of each pulsar, and which stays remarkably stable over time. This averaged profile is then used as a template, and the times-of-arrival (TOAs) of the individual pulses are then obtained by a least square fit.[3] As a result, for the Hulse–Taylor binary pulsar most of the data taken after 1981 have an uncertainty on the TOAs of about 20 μs or less. This

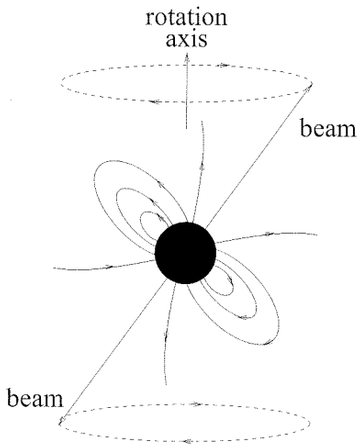

Fig. 6.2 The pulsar magnetosphere and the outgoing beams of radiation.

[3] In many cases (including the Hulse–Taylor binary pulsar) individual pulses are too weak to be detected. Then, one first forms an average over a few minutes of data, until it emerges a profile with a signal-to-noise ratio sufficiently large to be detectable. For the Hulse–Taylor binary pulsar this is performed integrating over about 5 minutes of data, which is a duration small enough compared to the orbital period, so the signal still refers to a localized position of the pulsar along its orbit and the modulation effects that we will discuss below are unimportant, but still is large enough so that a detectable signal emerges. The average over many blocks gives the standard profile used as a template. Matching the template against the average profile of each block gives an arrival time for a pulse near the middle of each block (see Taylor and Weisberg 1982).

precision is so good that it is possible to assign unambiguously a pulse number to each pulse, even after long periods in which observations have not been made; in particular, the Arecibo telescope was closed, for major upgrades, for various years in the mid 1990s, and still we know exactly how many pulses elapsed during that time, until observations resumed. This is quite remarkable if we consider that, with a rotation period of 59 ms, in one year there are about 5×10^8 pulses! It is this stability of the integrated profile that allows pulsars to be extraordinarily accurate clocks.

Even if a pulsars were, intrinsically, a perfect clock, the TOAs of the pulses in a earthbound laboratory will still be modulated by a number of time-dependent factors, due to the motion of the Earth around the Sun (and of the Sun around the solar system barycenter) and also by general-relativistic effects due to the gravitational field of the solar system. Furthermore, if a pulsar is a member of a binary system, the pulses will be similarly modulated by the motion of the pulsar around its companion, and by the strong gravitational fields of the two stars. These timing residuals, i.e. these modulations of the TOAs with respect to a perfectly periodic pattern, are a rich source of information, because they can be computed and depend on parameters of the binary system, such as the masses of the two stars, and therefore the measurement of the timing residual can allow us to determine these parameters. In the next subsections we will see how to compute this "timing formula", which takes into account all relevant corrections.

6.2.2 Roemer, Shapiro and Einstein time delays

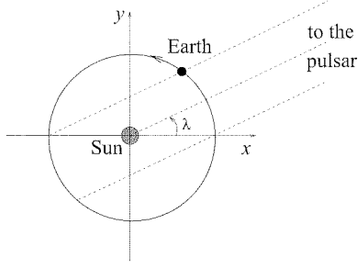

Fig. 6.3 The (x, y) plane is the plane of the orbit of the Earth around the Sun. The angle λ is the ecliptic longitude of the pulsar.

We consider a pulsar that emits a sequence of pulses, and we discuss first how the time of arrival of these pulses is modified by the motion of the Earth, and by the effect of the gravitational field of the solar system on electromagnetic waves. We will then see how these time of arrivals are affected if the pulsar is member of a binary system. Following a nomenclature originally introduced by Damour and Deruelle, we will split the corrections into three separate contributions, the Roemer, Shapiro and Einstein time delays.

Roemer time delay

Since light takes about 500 s to travel from the Sun to the Earth, there is an annual modulation of the time of arrivals. For instance, for a pulsar which is lying in the plane of the ecliptic, at ecliptic longitude λ, we see from Fig. 6.3 that this modulation is $\Delta_{R,\odot} = t_0 \cos(\Omega t - \lambda)$, where Ω is the angular velocity of the Earth around the Sun, t_0 is the travel time from the Sun to the Earth, and for simplicity we assumed a circular orbit. So, when the Earth is in the direction of the pulsar, $\Omega t - \lambda = 0$, the pulse arrives earlier, by an amount t_0, and when it is on the opposite side of the orbit, $\Omega t - \lambda = \pi$, it arrives later by an amount t_0, with respect to the arrival time at the Sun. This is called the Roemer time

delay.[4] The subscript R in $\Delta_{R,\odot}$ stands for Roemer, while $\odot$ reminds that this is a correction due to the motion of the observer, in the Solar System, and not to the intrinsic motion of the source.

If, rather than lying on the plane of the ecliptic, the pulsar has an ecliptic latitude β, the modulation is instead

$$\Delta_{R,\odot} = t_0 \cos(\Omega t - \lambda) \cos\beta \,. \tag{6.6}$$

Its amplitude is maximum for pulsars in the ecliptic plane, $\cos\beta = 0$, and vanishes for pulsars in the direction of the poles of the ecliptic. A variation $\delta\lambda, \delta\beta$ in the angles induces a variation of $\Delta_{R,\odot}$, given by

$$\delta(\Delta_{R,\odot}) = t_0 \, \delta\lambda \sin(\Omega t - \lambda) \cos\beta - t_0 \, \delta\beta \cos(\Omega t - \lambda) \sin\beta \,. \tag{6.7}$$

With a resolution $\delta t = 0.2$ ms on the arrival times of the pulses, and taking for definiteness an average angle $\beta \sim 45^0$, so $\sin\beta = \cos\beta = 1/\sqrt{2}$, we get an accuracy on the angles of order $\delta\lambda \sim \delta\beta \sim \sqrt{2}\,\delta t/t_0 \sim 5.6 \times 10^{-7}$ rad $\simeq 0.1$ arcsec. Such an accuracy can be sufficient to search for an optical counterpart. This is an example of the fact that the modulation of the originally periodic signal contains very useful information.

Actually, for pulsar timing we will need in general a better precision, so the orbit of the Earth cannot be approximated as circular. We must also take into account the rotation of the Earth around its axis, which for an Earth-bound laboratory introduces a daily modulation with an amplitude $R_\oplus/c \simeq 21$ ms, and we must even include the motion of the Sun around the solar system barycenter (which is determined primarily by the influence of Jupiter on the Sun, so that the solar system barycenter lies just outside the surface of the Sun). The most practical way to take into account these corrections is to refer all arrival times to the solar system barycenter (SSB). Let $\mathbf{r}_{\rm oe}$ be the vector from the observer to the center of the Earth, $\mathbf{r}_{\rm es}$ from the center of the Earth to the center of the Sun, and $\mathbf{r}_{\rm sb}$ from the center of the Sun to the SSB. Then the distance from the observer to the SSB is $\mathbf{r}_{\rm ob} = \mathbf{r}_{\rm oe} + \mathbf{r}_{\rm es} + \mathbf{r}_{\rm sb}$ and, to obtain the barycentric times of arrival, we must add to the times observed in the laboratory the quantity

$$\Delta_{R,\odot} = -\mathbf{r}_{\rm ob} \cdot \hat{\mathbf{n}}/c \,, \tag{6.8}$$

where $\hat{\mathbf{n}}$ is the unit vector from the SSB to the pulsar. The vectors $\mathbf{r}_{\rm oe}$, $\mathbf{r}_{\rm es}$ and $\mathbf{r}_{\rm sb}$ are known with sufficient accuracy (for $\mathbf{r}_{\rm es}$ it is also necessary to include the motion of the barycenter of the Earth–Moon system), so we can get $\hat{\mathbf{n}}$ from a measure of $\Delta_{R,\odot}$.

It should be remarked that the barycentric time of arrival so obtained are just a useful, but fictitious, intermediate quantity in our computation. The real time of arrival of the pulses at the SSB is also affected by other effects, such as the propagation of light in the gravitational field of the solar system and its interaction with the interstellar medium, as we will discuss below.

[4] After the Danish astronomer Ole Roemer who, in 1675, from the observation of Jupiter's moons, formulated the hypothesis that light travels at a finite speed. At that time the four largest moons of Jupiter were first observed when Jupiter is "in opposition", i.e. when the Earth passes between Jupiter and the Sun, since then Jupiter is high in the night sky and therefore easier to observe, and the times of the eclipses and passages (i.e. the passings of the moons behind and in front of Jupiter) could be predicted precisely. Later the moons of Jupiter were observed when the Earth was on the opposite side of the Sun from Jupiter, and it was found that the eclipses were consistently late by about 20 minutes. This led Roemer to the hypothesis that light propagates at a finite speed. His estimate for the speed of light was 214 000 km/s.

Shapiro time delay

The above computation of the Roemer delay neglected the general-relativistic effects of the gravitational field of the solar system on the propagation of light. To take it into account we recall, from eq. (5.11), that the space-time interval generated by a weak and nearly static Newtonian source can be written, to linear order in the metric perturbation ϕ, as

$$ds^2 = -[1 + 2\phi(\mathbf{x})]c^2dt^2 + [1 - 2\phi(\mathbf{x})]d\mathbf{x}^2 \,. \tag{6.9}$$

In the solar system, $|\phi(\mathbf{x})|$ is at most of order 10^{-6}, and the weak-field approximation is excellent. Photons travel along the light-like geodesic $ds^2 = 0$, so to lowest order in ϕ,

$$cdt = \pm[1 - 2\phi(\mathbf{x})]\,|d\mathbf{x}| \,. \tag{6.10}$$

If we denote by $\mathbf{r}_p$ the (fixed) position of the pulsar, and by $\mathbf{r}_{\rm obs}$ the position of the observer at the arrival time $t_{\rm obs}$, then the *coordinate* time difference, between the arrival time $t_{\rm obs}$ at the observer and the emission time at the pulsar t_e is

$$\begin{aligned} c(t_{\rm obs} - t_e) &= \int_{\mathbf{r}_{\rm obs}}^{\mathbf{r}_p} |d\mathbf{x}|\,[1 - 2\phi(\mathbf{x})] \\ &= |\mathbf{r}_p - \mathbf{r}_{\rm obs}| - 2\int_{\mathbf{r}_{\rm obs}}^{\mathbf{r}_p} |d\mathbf{x}|\,\phi(\mathbf{x}) \,. \end{aligned} \tag{6.11}$$

We write

$$\begin{aligned} |\mathbf{r}_p - \mathbf{r}_{\rm obs}| &= |(\mathbf{r}_p - \mathbf{r}_b) + (\mathbf{r}_b - \mathbf{r}_{\rm obs})| \\ &\simeq |\mathbf{r}_p - \mathbf{r}_b| + (\mathbf{r}_b - \mathbf{r}_{\rm obs}) \cdot \hat{\mathbf{n}} \,, \end{aligned} \tag{6.12}$$

where $\mathbf{r}_b$ is the position of the SSB, $\hat{\mathbf{n}}$ is the unit vector from the SSB to the pulsar, i.e. $\hat{\mathbf{n}} = (\mathbf{r}_p - \mathbf{r}_b)/|\mathbf{r}_p - \mathbf{r}_b|$, and the expansion in the second line is valid because $|\mathbf{r}_p - \mathbf{r}_b| \gg |\mathbf{r}_b - \mathbf{r}_{\rm obs}|$. Therefore, denoting $\mathbf{r}_b - \mathbf{r}_{\rm obs} \equiv \mathbf{r}_{\rm ob}$,

$$t_{\rm obs} \simeq \left(t_e + \frac{1}{c}|\mathbf{r}_p - \mathbf{r}_b|\right) + \frac{1}{c}\mathbf{r}_{\rm ob} \cdot \hat{\mathbf{n}} - \frac{2}{c}\int_{\mathbf{r}_{\rm obs}}^{\mathbf{r}_p} |d\mathbf{x}|\,\phi(\mathbf{x}) \,. \tag{6.13}$$

The term $t_e + |\mathbf{r}_p - \mathbf{r}_b|/c$ is the barycentric time of arrival, $t_{\rm SSB}$, defined as the (fictitious) time at which the pulse would arrive at the SSB if there were no effect of the gravity of the solar system. Then we get

$$t_{\rm SSB} = t_{\rm obs} - \frac{1}{c}\mathbf{r}_{\rm ob} \cdot \hat{\mathbf{n}} + \frac{2}{c}\int_{\mathbf{r}_{\rm obs}}^{\mathbf{r}_p} |d\mathbf{x}|\,\phi(\mathbf{x}) \,. \tag{6.14}$$

The first correction is just the Roemer time delay that we already found in eq. (6.8). The second term, which takes into account the effect on light propagation due to the gravitational potential of the solar system, is called (minus) the solar system Shapiro time delay,

$$\Delta_{S,\odot} = -\frac{2}{c}\int_{\mathbf{r}_{\rm obs}}^{\mathbf{r}_p} |d\mathbf{x}|\,\phi(\mathbf{x}) \,, \tag{6.15}$$

so

$$t_{\rm SSB} = t_{\rm obs} + \Delta_{R,\odot} - \Delta_{S,\odot} \,. \tag{6.16}$$

The Shapiro time delay is dominated by the gravitational field of the Sun. To compute it, we consider a photon emitted by the pulsar, which reaches the observer on the Earth when the pulsar–Sun–Earth angle has the value θ, see Fig. 6.4. Let P be a generic point on the straight-line trajectory made by the photon, and denote by ρ the distance of P from the Earth and by r its distance from the Sun. If $r_{\rm es} = 1$ au is the distance between the Earth and the Sun, we see from the figure that

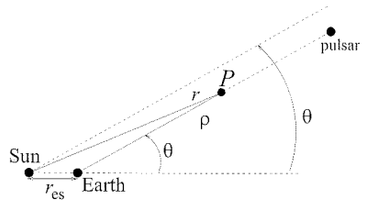

Fig. 6.4 The geometry for the computation of the Shapiro delay discussed in the text.

$$r^2 = (r_{\rm es} + \rho\cos\theta)^2 + (\rho\sin\theta)^2 \,, \tag{6.17}$$

i.e.

$$r = r_{\rm es}(u^2 + 1 + 2u\cos\theta)^{1/2} \,, \tag{6.18}$$

where $u = \rho/r_{\rm es}$. Since $\phi = (1/c^2)(-GM_\odot/r)$, we have

$$\begin{aligned} \Delta_{S,\odot} &= \frac{2GM_\odot}{c^3}\int_0^d \frac{d\rho}{r} \\ &= \frac{2GM_\odot}{c^3}\int_0^{\bar u} \frac{du}{(u^2 + 1 + 2u\cos\theta)^{1/2}} \,, \end{aligned} \tag{6.19}$$

where $\bar u = d/r_{\rm es}$, and d is the Earth–pulsar distance. It is convenient to add and subtract the delay at a given angle, say when $\cos\theta = 0$, so

$$\begin{aligned} \Delta_{S,\odot} = &\frac{2GM_\odot}{c^3}\int_0^{\bar u} \frac{du}{(u^2+1)^{1/2}} \\ &+ \frac{2GM_\odot}{c^3}\int_0^{\bar u} du\left[\frac{1}{(u^2 + 1 + 2u\cos\theta)^{1/2}} - \frac{1}{(u^2+1)^{1/2}}\right] . \end{aligned} \tag{6.20}$$

The term in the first line is a fixed quantity which, for $d/r_{\rm es}$ large, grows logarithmically,

$$\begin{aligned} \frac{2GM_\odot}{c^3}\int_0^{\bar u} \frac{du}{(u^2+1)^{1/2}} &= \frac{2GM_\odot}{c^3}\,{\rm arcsinh}(\bar u) \\ &\simeq \frac{2GM_\odot}{c^3}\log(2d/r_{\rm es}) \,. \end{aligned} \tag{6.21}$$

This is a constant shift that simply adds up to the total travel time from the pulsar to the SSB. The term in the second line is more interesting from our purposes, since it depends on θ, and therefore on the position of the Earth in its orbit around the SSB. In the integral in the second line of eq. (6.20) we can take the limit $\bar u = d/r_{\rm es} \to \infty$. The integral converges and gives

$$\int_0^\infty du\left[\frac{1}{(u^2 + 1 + 2u\cos\theta)^{1/2}} - \frac{1}{(u^2+1)^{1/2}}\right] = -\log(1 + \cos\theta) \,. \tag{6.22}$$

Thus, we get

$$\Delta_{S,\odot} = \frac{2GM_\odot}{c^3}\log\left(\frac{2d}{r_{\rm es}}\right) - \frac{2GM_\odot}{c^3}\log(1 + \cos\theta) \,. \tag{6.23}$$

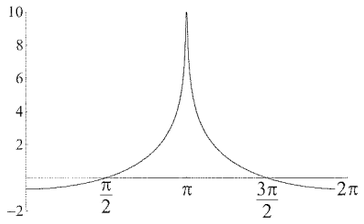

Fig. 6.5 The function $f(\theta) = -\log(1+\cos\theta)$, against θ.

A plot of the function $-\log(1+\cos\theta)$ is shown in Fig. 6.5. Observe that $\Delta_{S,\odot}$ formally diverges when $\theta = \pi$, that is, when the signal crosses the center of the Sun before reaching the Earth. However, of course, this divergence is fictitious, first of all because in this case the signal is simply absorbed by the Sun and second, because the Newtonian potential of the Sun is $-GM/r$ only outside the Sun, so the result is valid only for photons that at most graze the surface of the Sun.

Recalling that $2GM_\odot/c^2 \equiv R_{S,\odot} \simeq 3$ km is the Schwarzschild radius of the Sun, we see that the time-scale of the solar system Shapiro delay is given by the time that light takes to go across a distance $R_{S,\odot}$, that is, about $10\,\mu$s, which however is multiplied by large logarithmic factors. In particular, for a pulse which is just grazing the surface of the Sun, $\theta = \theta_{\rm grazing} \simeq \pi - (R_\odot/r_{\rm es})$, so $1+\cos\theta \simeq (1/2)(R_\odot/r_{\rm es})^2$. Then the maximum modulation induced by the Shapiro delay, i.e. the difference between its value for a pulse which is just grazing the Sun and its value at $\theta = 0$ is

$$\Delta_{S,\odot}(\theta = \theta_{\rm grazing}) - \Delta_{S,\odot}(\theta = 0) = \frac{4GM_\odot}{c^3}\log\frac{2r_{\rm es}}{R_\odot} \simeq 119.5\,\mu s\,. \tag{6.24}$$

It is also useful to rewrite eq. (6.23) as

$$\Delta_{S,\odot} = \frac{2GM_\odot}{c^3}\left[\log\left(\frac{d}{r_{\rm es}}\right) - \log\left(\frac{1+\cos\theta}{2}\right)\right]\,, \tag{6.25}$$

which stresses that $\Delta_{S,\odot}$ is the sum of two positive terms, given that $0 \leqslant (1+\cos\theta)/2 \leqslant 1$, and therefore its logarithm is negative. Therefore, $\Delta_{S,\odot} > 0$ for all values of θ. Since eq. (6.16) gives $t_{\rm obs} = (t_{\rm SSB} - \Delta_{R,\odot}) + \Delta_{S,\odot}$, we see that a positive $\Delta_{S,\odot}$ produces a *delay* in the time at which the pulse arrives at the observer (or at the SSB). This is physically correct, since the radio wave is delayed by the fact that it goes into the "potential well" in space-time generated by the presence of the Sun.

Einstein time delay

The Roemer and Shapiro time delays that we have computed are shifts in the *coordinate* time t. However, this is not the same as the time recorded by a clock in a laboratory. A laboratory clock located at a position $\mathbf{x}_{\rm obs}$ rather measures its own *proper* time τ, which in the metric (6.9) is related to t by

$$c^2 d\tau^2 = [1 + 2\phi(\mathbf{x}_{\rm obs})]c^2dt^2 - [1 - 2\phi(\mathbf{x}_{\rm obs})]d\mathbf{x}_{\rm obs}^2\,, \tag{6.26}$$

so, to first order in the small parameters $\phi(\mathbf{x}_{\rm obs})$ and $\mathbf{v}_{\rm obs} = d\mathbf{x}_{\rm obs}/dt$, we have

$$\frac{d\tau}{dt} \simeq 1 + \phi(\mathbf{x}_{\rm obs}) - \frac{v_{\rm obs}^2}{2c^2}\,. \tag{6.27}$$

Physically, the term $(-1/2)v_{\rm obs}^2/c^2$ gives the transverse Doppler shift, while ϕ gives the gravitational redshift. Integrating, we get

$$\tau \simeq t + \int^t dt'\,\left[\phi(\mathbf{x}_{\rm obs}(t')) - \frac{v_{\rm obs}^2(t')}{2c^2}\right]\,, \tag{6.28}$$

where the lower limit of the integral is arbitrary, since it corresponds to an arbitrary constant shift in the origin of τ. We can rewrite this as

$$t \simeq \tau + \Delta_{E\odot}\,, \tag{6.29}$$

where

$$\Delta_{E\odot} = \int^t dt'\,\left[\frac{v_{\rm obs}^2(t')}{2c^2} - \phi(\mathbf{x}_{\rm obs}(t'))\right]\,. \tag{6.30}$$

This is called the Einstein time delay. The dominant effect on $v_{\rm obs}$ comes from the motion of the Earth around the Sun, with velocity $v_\oplus$, and the rotation of the Earth around its axis gives a small correction, so we write $v_{\rm obs} \simeq v_\oplus$. We take the Earth in an elliptic orbit around the Sun, with semimajor axis a. Recall from eq. (4.53) that in a Keplerian orbit the total kinetic plus potential energy of the Earth–Sun system is related to the semimajor axis a by

$$E = -\frac{GM\mu}{2a}\,, \tag{6.31}$$

where μ is the reduced mass of the Earth–Sun system (i.e. the Earth mass, with excellent accuracy) and M the total mass (i.e. $M \simeq M_\odot$, with excellent accuracy). Since, on the other hand,

$$E = \frac{1}{2}\mu v_\oplus^2 - \frac{GM\mu}{r}\,, \tag{6.32}$$

we have

$$\frac{1}{2}v_\oplus^2 = \frac{GM_\odot}{r} - \frac{GM_\odot}{2a}\,, \tag{6.33}$$

and

$$\frac{d\Delta_{E\odot}}{dt} \simeq \frac{v_\oplus^2}{2c^2} - \phi = \frac{2GM_\odot}{c^2}\left(\frac{1}{r} - \frac{1}{4a}\right)\,. \tag{6.34}$$

A constant part in this expression is incorporated in the definition of atomic time, which is defined as the time measured by an atomic clock at a fixed distance a from the Sun. The dependence on r however introduces a modulation, due to the ellipticity of the Earth orbit.

Dispersion in the interstellar medium

Beside the Roemer, Shapiro and Einstein delays, which are due to the motion of the observer and to the gravitational field of the solar system, there is also a correction to the arrival times which is due to the propagation of the radio waves through the ionized interstellar gas, which effectively acts as a medium with a refraction index appreciably different from unity, and with an important frequency dependence. As a result, the component of the radio pulse with frequency ν travels with a group velocity v_g given by

$$v_g \simeq c\left(1 - \frac{n_e e^2}{2\pi m_e}\frac{1}{\nu^2}\right)\,, \tag{6.35}$$

where e and m_e are the charge and the mass of the electron, and n_e is the electron number density. The travel time over a distance L is therefore

$$\int_0^L \frac{dl}{v_g} \simeq \frac{L}{c} + \frac{1}{\nu^2}\left(\frac{e^2}{2\pi m_e c}\right)\int_0^L n_e dl\,. \tag{6.36}$$

The quantity

$$\mathrm{DM} \equiv \int_0^L n_e dl \tag{6.37}$$

is called the dispersion measure, and is typically quoted in cm^{-3} pc. Measuring the TOAs at different frequencies, we can get the dispersion measure, and we can correct for this effect. This procedure, known as de-dispersion, is performed separating the useful bandwidth of the receiver into many channels, such that in each channel the effect of dispersion is negligible. The output of the channels operating at different frequencies is then automatically corrected and superimposed, in order to enhance the signal-to-noise ratio.

To have an idea of the size of the effect, we observe that the Hulse–Taylor binary pulsar has a (relatively large) dispersion measure DM $\simeq 169\,\mathrm{cm}^{-3}$ pc. The measurements at Arecibo which led to its discovery were performed near 430 MHz. In the typical 4 MHz bandwidth around 430 MHz, this value of DM produces a spreading of the pulse of about 70 ms, which is larger than the intrinsic period of the pulsar of 59 ms, and the signal would then be unobservable. Thus, de-dispersion is a crucial part of pulsar observations. If one is performing a search for unknown pulsars, the value of DM is an unknown parameter, and the data are de-dispersed with various possible values of DM within a plausible range, i.e. DM becomes one of the dimensions of the parameter space in which data analysis is performed.

Relation to the intrinsic pulsar signal

We can now put together all these corrections. Since they are small, we can simply add them up linearly (e.g. the effect of the Einstein time delay on the Shapiro delay is totally negligible). Equation (6.30) shows that the time $\tau_{\rm obs}$ actually measured by a clock in a laboratory (i.e. its proper time) is related to the coordinate time $t_{\rm obs}$ by $t_{\rm obs} = \tau_{\rm obs} + \Delta_{E\odot}$, which, combined with eq. (6.16), gives

$$t_{\rm SSB} = \tau_{\rm obs} + \Delta_{E\odot} + \Delta_{R,\odot} - \Delta_{S,\odot}\,. \tag{6.38}$$

From this, we must still subtract the time delay due to the interaction with the interstellar medium, given in eq. (6.36), so we write

$$t_{\rm SSB} = \tau_{\rm obs} - \frac{D}{\nu^2} + \Delta_{E\odot} + \Delta_{R,\odot} - \Delta_{S,\odot}\,, \tag{6.39}$$

where

$$D = \left(\frac{e^2}{2\pi m_e c}\right)\mathrm{DM}\,. \tag{6.40}$$

The quantity $t_{\rm SSB}$ so obtained is the coordinate time at which the signal recorded by our laboratory clock at $\tau_{\rm obs}$ would have arrived at a fixed point in space such as the solar system barycenter, if there were no effect due to the gravitational potential of the solar system, and no interaction with the interstellar medium. It therefore depends only on the intrinsic properties of the source.

The emission mechanism of the pulsar is not yet completely understood, but in any case is believed to be related to some "hot spot" corotating with the pulsar. If we denote by Φ the accumulated phase of the spinning pulsar, and we neglect for the moment any proper motion of the pulsar, we see a pulse whenever the phase Φ goes back to the same value Φ_0, mod 2π, at which the radiated beam sweeps across the Earth. If we denote by T the proper time in the pulsar frame, for a perfectly periodic pulsar, spinning with frequency ν, we would have $\Phi = 2\pi\nu T$. Actually, ν cannot be exactly constant. In particular, the pulsar must spin down because the energy of the beam is ultimately taken from its rotational energy (and also, because any deviation of axisymmetry leads to a production of gravitational waves, as we saw in Section 4.2). We can model phenomenologically the evolution of the pulsar frequency performing a Taylor expansion around some reference value $T_0 = 0$ of the pulsar proper time,

$$\nu(T) = \nu_0 + \dot\nu_0 T + \frac{1}{2}\ddot\nu_0 T^2 + \ldots\,, \tag{6.41}$$

where $\dot\nu_0, \ddot\nu_0$, etc. are generically called the spindown parameters. Then the accumulated phase is given by

$$\begin{aligned}\frac{1}{2\pi}\Phi(T) &= \int_0^T d\tau\,\nu(\tau) \\ &= \nu_0 T + \frac{1}{2}\dot\nu_0 T^2 + \frac{1}{6}\ddot\nu_0 T^3 + \ldots\,.\end{aligned} \tag{6.42}$$

Emission will take place at the proper times T_n such that $\Phi(T_n) = \Phi_0 + 2\pi n$. Then the emission proper times T_n are given by

$$\nu_0 T_n + \frac{1}{2}\dot\nu_0 T_n^2 + \frac{1}{6}\ddot\nu_0 T_n^3 + \ldots = n + \frac{\Phi_0}{2\pi}\,, \tag{6.43}$$

so the spindown parameters produce deviations from the exact periodicity $T_n = (\Phi_0/2\pi\nu_0) + (1/\nu_0)n$. The typical dissipation mechanisms in pulsars produce a power-like behavior $\dot\nu \simeq C\nu^n$, with C a constant and $n \sim 2-3$ (or at most $n = 5$ for damping due to GW emission, see eq. (4.228)). This gives $\ddot\nu \simeq Cn\nu^{n-1}\dot\nu = n\dot\nu^2/\nu$. For the Hulse–Taylor pulsar, $\nu_0 \simeq 16.9\,\mathrm{s}^{-1}$ and $\dot\nu_0 \simeq -2.5\times10^{-15}\,\mathrm{s}^{-2}$, so one expects a value of the second derivative of order $\ddot\nu_0 \simeq 3\times10^{-31}\,\mathrm{s}^{-3}$, which over the time span of the observation is unobservably small. Thus, in this case it is sufficient to keep only $\dot\nu_0$ in eq. (6.41).

This model assumes that the evolution of the pulsar frequency is smooth. Actually, most pulsars exhibit "glitches" , i.e. sudden jumps in their rotational periods, related to some form of rearrangement of their

internal structure. For instance, the Vela pulsar typically has glitches at intervals of about three years, where the period sudden decreases up to 200 ns (for comparison, the normal rate of change of the period of the Vela pulsar is an increase by about 10 ns/day). However, the Hulse–Taylor pulsar has shown a remarkable stability, and no glitches, over the 30 years period that is has been observed.

The final step is to connect the pulsar proper time T with the coordinate time t. This will give the values of coordinate time at emission, $t_{\mathrm{em},n} = t(T_n)$; apart from corrections due to the pulsar proper motion, to be discussed below, we can then trivially compute the barycentric time of arrivals $t_{\mathrm{SSB},n}$, i.e. the fictitious values of coordinate time at which these signals would arrive at the solar system barycenter in the absence of dispersion and of Shapiro delay: these are simply $t_{\mathrm{SSB},n} = t_{\mathrm{em},n} + d/c$, where d is the distance between the barycenter of the pulsar–companion system and the SSB. Thus, once we compute the relation between proper time T and the coordinate time t, which we will do in the next subsection, both the time of arrivals measured by our laboratory clock and the timing predicted by this pulsar model have been expressed in terms of the same variable, t_{SSB}, and can be compared.

6.2.3 Relativistic corrections for binary pulsars

For a pulsar in a binary system we can proceed similarly to what we have done for the Earth–Sun system, and perform the transformation from the pulsar proper time to the coordinate time of the pulsar–companion barycenter. We therefore have also Roemer, Shapiro and Einstein delays associated to the pulsar–companion system. The crucial difference, however, with respect to the solar system corrections, is that the binary pulsar is a fairly relativistic system, with strong gravitational fields, and therefore general-relativistic effects are much more important. This is a blessing, since it is just this fact that allows us to measure general-relativistic effects in such systems, such as the emission of gravitational radiation, but it also implies that the computation is technically more difficult, since a full general-relativistic treatment of the two-body dynamics becomes necessary. We discuss the various relevant effects in turn.[5]

[5] It should be observed that the splitting of the various contribution to the timing formula into Einstein, Roemer and Shapiro time delays, aberration delays, etc. discussed below, is not invariant under general coordinate transformations, so it really refers to the harmonic coordinate system, in which the interval has the form (6.9).

Einstein time delay

For this term, the Newtonian equation of the trajectory gives a sufficient accuracy. The computation is therefore similar to what we did on page 310, except that in the expressions for the reduced and total mass of the system we must use the masses m_p and m_c of the pulsar and of its companion. There is however a subtle conceptual point. The beam is radiated by some "hot spot" at a position $\mathbf{x}$ on the surface of the pulsar. The Newtonian expression for ϕ at the location $\mathbf{x}$ is

$$\phi(\mathbf{x}) = -\frac{Gm_p}{c^2|\mathbf{x}-\mathbf{x}_p|} - \frac{Gm_c}{c^2|\mathbf{x}-\mathbf{x}_c|}\,, \tag{6.44}$$

where $\mathbf{x}_p$ is the position of the center of the pulsar and $\mathbf{x}_c$ is the position of the companion. Using the numerical values in eqs. (6.1) and (6.2), the second term is of order $Gm_c/(c^2a) \sim 10^{-6}$ and therefore is small. For this term, therefore, the weak-field approximation is legitimate. The self-gravity of the pulsar however is strong on its surface. For a typical neutron star radius $r_{NS} \simeq 10$ km and $m_p \simeq 1.4M_\odot$, we have $Gm_p/(c^2 r_{NS}) \simeq 0.2$. However, this term (as well as its generalization in full general relativity) does not change along the trajectory of the pulsar in orbit around its companion, so it does not introduce a modulation of the time of arrivals. Its effect is simply reabsorbed in a constant rescaling of proper time T, which is not observable.[6] Thus, the time-dependent part of the Einstein time delay can be computed simply using

[6] A more detailed discussion on this point can be found in Will (1984).

$$\phi(\mathbf{x}) = -\frac{Gm_c}{c^2|\mathbf{x}-\mathbf{x}_c|}\,, \tag{6.45}$$

and the weak field approximation. Then, eq. (6.27) gives

$$\frac{dT}{dt} = 1 - \frac{Gm_c}{c^2|\mathbf{x}_p-\mathbf{x}_c|} - \frac{v_p^2}{2c^2}\,, \tag{6.46}$$

where $\mathbf{x}_p$ is the pulsar position and v_p is its velocity. The latter is obtained from

$$v_p = \frac{m_c}{m_p+m_c}\,v\,, \tag{6.47}$$

where v is the relative velocity in the center of mass system, given by (compare with eq. (6.33))

$$\frac{1}{2}v^2 - \frac{G(m_p+m_c)}{r} = -\frac{G(m_p+m_c)}{2a}\,, \tag{6.48}$$

Thus,

$$\frac{dT}{dt} = 1 - \frac{G}{c^2}\left[\frac{m_c(m_p+2m_c)}{m_p+m_c}\,\frac{1}{r} - \frac{m_c^2}{m_p+m_c}\,\frac{1}{2a}\right]. \tag{6.49}$$

We use the parametrization of the Keplerian orbit in terms of the eccentric anomaly u, given in eqs. (4.56) and (4.57), with u related to the time t by Kepler equation (4.58),

$$u - e\sin u = \frac{2\pi}{P_b}\,(t-t_0)\,, \tag{6.50}$$

where t_0 is a reference time of periastron passage. Differentiating, we have

$$\frac{du}{dt}\,(1-e\cos u) = \frac{2\pi}{P_b}\,, \tag{6.51}$$

and therefore,

$$\frac{dT}{dt} = \frac{du}{dt}\,\frac{dT}{du} = \frac{2\pi}{P_b}\,\frac{1}{1-e\cos u}\,\frac{dT}{du}\,. \tag{6.52}$$

Plugging this into eq. (6.49) and using eq. (4.56) we get

$$\begin{aligned}\frac{2\pi}{P_b}\frac{dT}{du} &= \left(1-\frac{G}{c^2}\frac{2m_cm_p+3m_c^2}{2a(m_p+m_c)}\right)-e\cos u\left(1+\frac{G}{c^2}\frac{m_c^2}{2a(m_p+m_c)}\right)\\ &\simeq \left(1-\frac{G}{c^2}\frac{2m_cm_p+3m_c^2}{2a(m_p+m_c)}\right)\\ &\quad\times\left[1-e\cos u\left(1+\frac{G}{c^2}\frac{m_c(m_p+2m_c)}{a(m_p+m_c)}\right)\right],\end{aligned}\tag{6.53}$$

where in the second line we retained only terms of first order in G. The overall factor is a constant multiplicative rescaling of the pulsar proper time T. Such a factor is unobservable, since it relates the (unobservable) proper time that the pulsar would have in the presence of only its own gravitational field, to its actual proper time that includes the gravitational effect of the companion and the pulsar orbital velocity. Instead, the correction proportional to $\cos u$ produces a modulation along the orbit and is therefore observable. We can therefore reabsorb the multiplicative factor into the definition of proper time, rescaling

$$T\to\left(1-\frac{G}{c^2}\frac{2m_cm_p+3m_c^2}{2a(m_p+m_c)}\right)T\,,\tag{6.54}$$

and eq. (6.53) becomes

$$\frac{dT}{du}=\frac{P_b}{2\pi}\left(1-e\cos u\right)-\gamma\cos u\tag{6.55}$$

where the Einstein parameter γ is given by

$$\begin{aligned}\gamma &= e\left(\frac{P_b}{2\pi}\right)\frac{G}{c^2}\frac{m_c(m_p+2m_c)}{a(m_p+m_c)}\\ &= e\left(\frac{P_b}{2\pi}\right)^{1/3}\frac{G^{2/3}}{c^2}\frac{m_c(m_p+2m_c)}{(m_p+m_c)^{4/3}}\,,\end{aligned}\tag{6.56}$$

and in the second line we used Kepler's law, $G(m_p+m_c)/a^3=(2\pi/P_b)^2$, to eliminate a. Writing $T=t-\Delta_E$, and observing, from eq. (6.50), that $(2\pi/P_b)dt/du=1-e\cos u$, we see that

$$\frac{d\Delta_E}{du}=\gamma\cos u\,.\tag{6.57}$$

Then, we obtains for the Einstein delay

$$\Delta_E=\gamma\sin u\,.\tag{6.58}$$

Inserting the numerical values of e and P_b of the Hulse–Taylor pulsar, eq. (6.56) gives

$$\gamma=2.93696\,\mathrm{ms}\left(\frac{m_c}{M_\odot}\right)\left(\frac{m_p+2m_c}{M_\odot}\right)\left(\frac{m_p+m_c}{M_\odot}\right)^{-4/3}.\tag{6.59}$$

Roemer time delay and the post-Newtonian orbit

Referring the emission time to the barycenter of the pulsar–companion system, we encounter the Roemer and Shapiro time delays, similarly to what we found for the solar system corrections. In the geometry of Fig. 6.1, the Roemer delay is given by $\Delta_R=\hat{\mathbf{z}}\cdot\mathbf{x}_1(t)/c$, where $\mathbf{x}_1$ is the distance of the pulsar from the center-of-mass of the pulsar–companion system. We therefore need the explicit form of the orbit, $\mathbf{x}_1(t)$.

We first consider a Keplerian orbit, neglecting general-relativistic corrections. Using polar coordinates (r_1,ψ) in the plane of the orbit, the Keplerian equation of motion is given in parametric form, in terms of the eccentric anomaly u, by

$$r_1(u)=a_1[1-e\cos u]\,,\tag{6.60}$$

$$\cos\psi(u)=\frac{\cos u-e}{1-e\cos u}\tag{6.61}$$

(compare with eqs. (4.56) and (4.57)), where a_1 is the semimajor axis of the pulsar orbit. Observe that r_1 reaches its minimum value at $u=0$, in which case $\psi=0$. Therefore the angle ψ is measured from periastron, and the angle measured from the line of nodes is $\omega+\psi(u)$, see Fig. 6.1. From the geometry of Fig. 6.1 we then see that the Roemer delay is

$$\Delta_R=r_1(u)\sin\iota\sin[\omega+\psi(u)]\,.\tag{6.62}$$

We now expand $\sin(\omega+\psi)=\cos\psi\sin\omega+\sin\psi\cos\omega$ and we use eq. (6.61) for $\cos\psi$, together with the corresponding expression for $\sin\psi$,

$$\sin\psi(u)=(1-e^2)^{1/2}\frac{\sin u}{1-e\cos u}\,,\tag{6.63}$$

and we get

$$\begin{aligned}\Delta_R &= \frac{r_1(u)}{1-e\cos u}\sin\iota[(\cos u-e)\sin\omega+(1-e^2)^{1/2}\sin u\cos\omega]\\ &= a_1\sin\iota[(\cos u-e)\sin\omega+(1-e^2)^{1/2}\sin u\cos\omega]\,.\end{aligned}\tag{6.64}$$

This is the result at the Keplerian level. However, numerically the effect is quite large, and it is necessary to go beyond the Keplerian orbit, and include the post-Newtonian corrections to 1PN order. This computation has been performed by Damour and Deruelle (1985, 1986), and we sketch the main steps. The equations of motion at 1PN level can be derived from the Lagrangian (5.54). Defining the variable

$$\mathbf{X}=\frac{m_1^*\mathbf{x}_1+m_2^*\mathbf{x}_2}{m_1^*+m_2^*}\,,\tag{6.65}$$

where

$$m_A^*=m_A+\frac{m_Av_A^2}{2c^2}-\frac{Gm_1m_2}{2rc^2}\,,\tag{6.66}$$

the equations of motion give $d^2\mathbf{X}/dt^2=0$. In the non-relativistic limit this is the statement that the center-of-mass is non accelerated. In fact, because of the corrections $O(v^2/c^2)$, $\mathbf{X}$ is rather a "center-of-energy".

Invariance under time translations and rotations leads to the conservation of energy and angular momentum. Because of conservation of angular momentum, the equation for the relative coordinate $\mathbf{r}$ describes a motion in a plane, just as in the Newtonian case, and there are two conserved quantities, the total energy E and the total angular momentum $\mathbf{J}$. We use the usual notations m for the total mass, $m = m_1 + m_2$, μ for the reduced mass $\mu = m_1 m_2/m$ and, as in Chapter 5, we use the symmetric mass ratio $\nu = \mu/(m_1 + m_2) = m_1 m_2/(m_1 + m_2)^2$ (observe that $0 \leqslant \nu \leqslant 1/4$). It is also convenient to introduce the energy and angular momentum per unit value of μ, $\varepsilon = E/\mu$, $\mathbf{j} = \mathbf{J}/\mu$. Applying the Noether theorem to the Lagrangian (5.54), one finds the explicit expression of the conserved quantities,

$$\varepsilon = \frac{1}{2}v^2 - \frac{Gm}{r} + \frac{3}{8}(1-3\nu)\frac{v^4}{c^2} + \frac{Gm}{2rc^2}\left[(3+\nu)v^2 + \nu(\hat{\mathbf{r}}\cdot\mathbf{v})^2 - \frac{Gm}{r}\right], \tag{6.67}$$

and

$$\mathbf{j} = \left[1 + \frac{1}{2}(1-3\nu)\frac{v^2}{c^2} + (3+\nu)\frac{Gm}{rc^2}\right]\mathbf{r}\times\mathbf{v}\,, \tag{6.68}$$

where v is the relative velocity and $\hat{\mathbf{r}} = \mathbf{r}/r$. Using polar coordinates (r,ψ) in the plane of the orbit, these first integrals of the equations of motion give

$$\left(\frac{dr}{dt}\right)^2 = A + \frac{2B}{r} + \frac{C}{r^2} + \frac{D}{r^3}\,, \tag{6.69}$$

$$\frac{d\psi}{dt} = \frac{H}{r^2} + \frac{I}{r^3}\,, \tag{6.70}$$

where $A,\ldots,I$ are polynomials in ε and j,

$$A = 2\varepsilon\left[1 + \frac{3}{2}(3\nu-1)\frac{\varepsilon}{c^2}\right], \tag{6.71}$$

$$B = Gm\left[1 + (7\nu-6)\frac{\varepsilon}{c^2}\right], \tag{6.72}$$

$$C = -j^2\left[1 + 2(3\nu-1)\frac{\varepsilon}{c^2}\right] + (5\nu-10)\frac{G^2m^2}{c^2}, \tag{6.73}$$

$$D = (8-3\nu)\frac{GMj^2}{c^2}, \tag{6.74}$$

$$H = j\left[1 + (3\nu-1)\frac{\varepsilon}{c^2}\right], \tag{6.75}$$

$$I = (2\nu-4)\frac{GMj}{c^2}. \tag{6.76}$$

In the limit $c\to\infty$ we have $D = I = 0$, while the other coefficients reduce to their Newtonian values. Observe that in the Newtonian case the equation for $(dr/dt)^2$ contains terms up to $1/r^2$, while at the 1PN level there is also a $1/r^3$ term, that in principle could make the integration of the equation of motion very complicated. However, as observed by Damour and Deruelle, we can introduce a new radial variable $\bar{r}$,

$$\bar{r} = r + \frac{D}{2j^2}\,, \tag{6.77}$$

and in terms of this variable eq. (6.69) becomes

$$\left(\frac{d\bar{r}}{dt}\right)^2 = A + \frac{2B}{\bar{r}} + \frac{\bar{C}}{\bar{r}^2} + O(v^4/c^4)\,, \tag{6.78}$$

with $\bar{C} = C + (BD/j^2)$. Since the terms $O(v^4/c^4)$ are consistently neglected at this order, this equation still has the form of a Newtonian-like radial equation of motion, with suitably redefined parameters. Similarly, defining $\tilde{r} = r - I/(2H)$, the angular equation (6.70) becomes

$$\frac{d\psi}{dt} = \frac{H}{\tilde{r}^2}\,. \tag{6.79}$$

As a result, the equations of motion to 1PN order can be integrated analytically, and the solution can be put in a form similar to the Keplerian orbit discussed in Section 4.1.2. In particular, eqs. (4.56) and (4.58) become

$$u - e_t\sin u = \frac{2\pi}{P_b}\,t\,, \tag{6.80}$$

and

$$r = a_r[1 - e_r\cos u]\,, \tag{6.81}$$

where

$$a_r = -\frac{Gm}{2\varepsilon}\left[1 - (\nu-7)\frac{\varepsilon}{2c^2}\right], \tag{6.82}$$

$$e_r^2 = 1 + \frac{2\varepsilon}{G^2m^2}\left[1 + (5\nu-15)\frac{\varepsilon}{2c^2}\right]\left[j^2 + (\nu-6)\frac{G^2m^2}{c^2}\right], \tag{6.83}$$

$$e_t^2 = 1 + \frac{2\varepsilon}{G^2m^2}\left[1 + (17-7\nu)\frac{\varepsilon}{2c^2}\right]\left[j^2 + (2-2\nu)\frac{G^2m^2}{c^2}\right], \tag{6.84}$$

$$\frac{2\pi}{P_b} = \frac{(-2\varepsilon)^{3/2}}{Gm}\left[1 - (\nu-15)\frac{\varepsilon}{4c^2}\right]. \tag{6.85}$$

In other words, the eccentricity e of the Keplerian solution is now split into a "radial eccentricity" e_r and a "time eccentricity" e_t. Similarly, the solution for $\psi(u)$ is written in terms of an "angular eccentricity" e_θ,

$$\psi = \omega_0 + (1+k)A_{e_\theta}(u)\,, \tag{6.86}$$

where[7]

$$k = \frac{3Gm}{c^2a(1-e^2)}\,. \tag{6.87}$$

The function $A_{e_\theta}(u)$ is the same as in eq. (4.61), with $e\to e_\theta$, and

$$e_\theta^2 = 1 + \frac{2\varepsilon}{G^2m^2}\left[1 + (\nu-15)\frac{\varepsilon}{2c^2}\right]\left[j^2 - 6\frac{G^2m^2}{c^2}\right]. \tag{6.88}$$

Observe that, when $c\to\infty$, e_θ^2, e_r^2 and e_t^2 reduce to the Keplerian quantity e^2 given in eq. (4.50). We therefore have a parametric "quasi-Newtonian" (i.e. Newtonian plus the precession due to a non-vanishing k in eq. (6.86)) representation of the orbit accurate to 1PN order.[8] Using

[7] Observe that, since k is already a correction, to the order at which we are working it is irrelevant whether in eq. (6.87) we write the Keplerian major semiaxis $a = -Gm/(2\varepsilon)$ rather than a_r, and similarly we can use e or any other eccentricity such as e_r.

[8] At the same time, the equation of motion (6.80) can be rewritten in terms of the proper time T of the pulsar, rather than in terms of coordinate time t, as

$$u - e_T\sin u = \frac{2\pi}{P_b}\,T\,, \tag{6.89}$$

where e_T is another time eccentricity. It is crucial to carefully distinguish between these time eccentricities to get the correct 1PN result. See Damour and Deruelle (1985, 1986) for details.

this expression for the orbit, eq. (6.64) is replaced by

$$\Delta_R = a_1 \sin\iota[(\cos u - e_r)\sin\omega + (1-e_\theta^2)^{1/2}\,\sin u\cos\omega]\,. \tag{6.90}$$

Writing $e_r = (1+\delta_r)e$ and $e_\theta = (1+\delta_\theta)e$, where e is the Keplerian eccentricity given by eq. (4.50), the parameters δ_r and δ_θ have the values

$$\delta_r = \frac{G}{c^2}\,\frac{3m_p^2+6m_pm_c+2m_c^2}{a(m_p+m_c)}\,, \tag{6.91}$$

$$\delta_\theta = \frac{G}{c^2}\,\frac{(7/2)m_p^2+6m_pm_c+2m_c^2}{a(m_p+m_c)}\,, \tag{6.92}$$

where we wrote $m_1 = m_p, m_2 = m_c$ for the masses of the pulsar and the companion.[9] Finally, we observe from eq. (6.81) that the periastron passages (i.e. the minima of r) are reached for $u = u_n \equiv 2\pi n$, with n integer. Since $A_{e_\theta}(u_n) = 2\pi n$, we see from eq. (6.86) that $2\pi k$ is the angle of periastron precession per orbit. Observe that, in the complete general-relativistic solution, the advance of the periastron is not uniform along the orbit, but is a function of u. Since the position ω of the periastron advances by $2\pi k$ over one period, the derivative of ω, averaged over the orbit, is

$$\begin{aligned}\langle\dot\omega\rangle &= \frac{2\pi}{P_b}k \\ &= \frac{3}{c^2}\,[G(m_p+m_c)]^{2/3}\,\left(\frac{2\pi}{P_b}\right)^{5/3}\,\frac{1}{1-e^2}\,,\end{aligned} \tag{6.93}$$

where in the second line we used eq. (6.87), and we eliminated a using Kepler's law. Using the known values of e and P_b for the Hulse–Taylor binary pulsar, this gives

$$\langle\dot\omega\rangle = 2.11353\,\left(\frac{m_p+m_c}{M_\odot}\right)^{2/3}\,\mathrm{deg/yr}\,. \tag{6.94}$$

The comparison with the experimental value therefore gives the total mass of the binary system.

Shapiro time delay

The Shapiro delay is due to the effect of the gravitational field of the companion on the pulsar signal (observe that the gravitational field of the pulsar itself enters instead in the relation between the pulsar proper time and coordinate time, just as the Earth's gravitational field when we computed the solar system corrections). The computation is analogous to what we did on pages 308–310. Using the Keplerian equation of the orbit given in eqs. (4.56) and (4.57), and taking into account its orientation with respect to the observer, given by the periastron angle ω and by the inclination angle ι, one obtains

$$\Delta_S = -2r\log\left\{(1-e\cos u) - s[\sin\omega(\cos u - e) + \sqrt{1-e^2}\,\cos\omega\sin u]\right\}, \tag{6.95}$$

[9] In all these equations we have assumed the correctness of general relativity. Alternatively, quantities such as δ_r and δ_θ can be treated as free parameters, to be determined directly from the data, and their measure allows us to compare general relativity to alternative theories of gravitation.

where $r \equiv Gm_c/c^3$ (not to be confused with a distance) and $s \equiv \sin\iota$ are called the range and shape of the Shapiro delay, respectively, and we omitted an overall constant (i.e., a u-independent term), which grows logarithmically with the distance to the pulsar. This constant term simply adds up to the total travel time, but it does not show up as a modulation in u, and is therefore unobservable.

Secular changes due to GW emission

The timing formula also includes secular changes in the Keplerian parameters of the orbit, induced by GW emission, whose extraction is in fact our final aim. In particular we already saw that, because of GW emission, the orbital period has a non-vanishing time derivative given by eq. (6.4).[10]

This secular change modifies the Keplerian relation (6.50) between the eccentric anomaly u and the proper time T of the pulsar, which becomes

$$u - e\sin u = 2\pi\left[\frac{T-T_0}{P_b} - \frac{1}{2}\dot P_b\left(\frac{T-T_0}{P_b}\right)^2\right], \tag{6.96}$$

where T_0 is a reference value of proper time, and P_b is defined as the value of the orbital period at this reference time. The factor $-1/2$ comes from integrating the instantaneous orbital frequency $[P_b + \dot P_b(T-T_0)]^{-1}$ to obtain the orbital phase.

Observe that, in order of magnitude, the velocity v of the binary system is given by $v^2 \sim GM/a$, where $M = m_p + m_c$ is the total mass. Using Kepler's law to eliminate a in favor of P_b, this can be rewritten as $P_b/(2\pi) \sim GM/v^3$. Substituting this into the expression for $\dot P_b$, given in eq. (6.4), we see that

$$\dot P_b = O\left(\frac{v^5}{c^5}\right)\,. \tag{6.97}$$

It is quite remarkable that an effect of order $(v/c)^5$ can be measured, and this is due to the combination of the extreme precision of the timing measurements, and to the fact that the Hulse–Taylor binary system is quite relativistic, with $v \sim 10^{-3}c$.

Aberration correction and Doppler shift

Another ingredient of the full timing formula is an aberration correction due to the fact that, because of the orbital motion of the pulsar around its companion, the direction from which the observer receives the pulse differs from the direction in which it was emitted in the pulsar frame. This produces a delay

$$\Delta_A = A\{\sin[\omega + A_e(u)] + e\sin\omega\} + B\{\cos[\omega + A_e(u)] + e\cos\omega\}\,, \tag{6.98}$$

where A and B are two known constants. Finally, there is a longitudinal Doppler shift, due to the fact that there is in general a proper motion of

[10] Actually, also $x = (1/c)a\sin\iota$ and the eccentricity e have secular changes, see eqs. (4.116) and (4.117), which however are smaller, and not detectable with the present precision for the Hulse–Taylor pulsar.

the solar system barycenter with respect to the barycenter of the pulsar–companion system, with a radial component of the velocity. Thus, the relation between the intrinsic and the observed orbital periods is given by

$$P_b^{\rm intr} = D P_b^{\rm obs} \,, \tag{6.99}$$

and the Doppler factor D is given by

$$D = \left(1 - \frac{\mathbf{v}\cdot\hat{\mathbf{n}}}{c}\right) , \tag{6.100}$$

where $\mathbf{v}$ is the velocity of the pulsar–companion barycenter with respect to the SSB, and $\hat{\mathbf{n}}$ is the unit vector from the SSB toward the pulsar. From eq. (6.99) we get

$$\frac{\dot{P}_b^{\rm obs}}{P_b^{\rm obs}} = \frac{\dot{P}_b^{\rm intr}}{P_b^{\rm intr}} - \frac{\dot{D}}{D} \,. \tag{6.101}$$

If the Doppler factor D were a constant in time, the additional term $\dot{D}/D$ would vanish, that is, D would be simply reabsorbed into the definition of P_b, and would be unobservable. However, there is a relative acceleration of the SSB and of the pulsar–companion system, induced by the differential rotation of the Galaxy, as well as proper motion effects, and therefore $\dot{D}$ is non-vanishing and produces an observable correction to $\dot{P}_b/P_b$. To lowest order in the radial velocity $\mathbf{v}\cdot\hat{\mathbf{n}}$, we have $\dot{D}/D \simeq \dot{D}$, and

$$\begin{aligned} -\dot{D} &= \frac{d}{dt}\frac{\mathbf{v}\cdot\hat{\mathbf{n}}}{c} \\ &= \frac{\mathbf{a}\cdot\hat{\mathbf{n}}}{c} + \frac{\mathbf{v}}{c}\cdot\frac{d\hat{\mathbf{n}}}{dt} \,. \end{aligned} \tag{6.102}$$

If the pulsar has a transverse velocity v_T with respect to the SSB, and as usual d is the distance to the pulsar, in a time dt the unit vector $\hat{\mathbf{n}}$ acquires a component $v_T dt/d$ in the transverse direction, and therefore $\mathbf{v}\cdot d\hat{\mathbf{n}}/dt = v_T^2/d$. Thus, there is a Doppler correction

$$\left(\frac{\dot{P}_b}{P_b}\right)^{\rm obs} = \left(\frac{\dot{P}_b}{P_b}\right)^{\rm intrinsic} + \left(\frac{\dot{P}_b}{P_b}\right)^{\rm gal} , \tag{6.103}$$

where $(\dot{P}_b/P_b)^{\rm gal}$ is the value of $-\dot{D}/D$ due to the galactic acceleration and to proper motion

$$\left(\frac{\dot{P}_b}{P_b}\right)^{\rm gal} = \frac{\mathbf{a}\cdot\hat{\mathbf{n}}}{c} + \frac{v_T^2}{c\,d} \,. \tag{6.104}$$

The term $v_T^2/(c\,d)$ is also known as the Shklovsky effect due to the orbital motion. For a pulsar in the galactic plane, eq. (6.104) can be rewritten as

$$\left(\frac{\dot{P}_b}{P_b}\right)^{\rm gal} = -\frac{v_0^2}{cR_0}\cos l - \frac{v_1^2}{cR_1}\cos\lambda + \frac{v_T^2}{c\,d} \,, \tag{6.105}$$

where v_0 is the galactic circular velocity at the Sun position, R_0 the distance from the galactic center to the Sun, v_1 and R_1 are respectively the galactic circular velocity and the distance to the galactic center at the pulsar position, l is the galactic latitude of the pulsar and λ the Sun-pulsar-galactic center angle.[11]

We see from eq. (6.37) that, if we have a model of the electron distribution in the Galaxy, we can get the distance of a pulsar from us from the observed value of its dispersion measure. For the Hulse–Taylor pulsar this gives

$$d = 8.3 \pm 1.4\,{\rm kpc} \,. \tag{6.106}$$

At this relatively large distance, the last term in eq. (6.105) is small, since it is proportional to $1/d$. However, the difference between the acceleration at the Earth and pulsar location, due to the differential rotation of the Galaxy, is quite important. Furthermore, this correction is sensitive to the values of v_0 and R_0, which are not very accurately known. Indeed, for the Hulse–Taylor the uncertainty in the first two terms in eq. (6.105) is the limiting factor in the comparison between the experimental results and the general relativity prediction.

[11] For a pulsar outside the galactic plane, there is also a (usually smaller) effect due to the vertical acceleration in the galactic potential. All these acceleration corrections are discussed in detail in Damour and Taylor (1991).

Fit to the full timing formula

At this point, one can compare these corrections with the observed timing residual and extract, from a fit, the parameters that enter in the timing formula. These parameters can be grouped as follows.

- Parameters characterizing the pulsar itself: the right ascension α and declination δ, its proper motion, the initial pulse phase Φ_0, its frequency ν and the spindown parameters. In practice, among the spindown parameters it suffices to keep only $\dot{\nu}_0$, as we saw below eq. (6.41).
- The five Keplerian parameters

$$\{P_b, T_0, x, e, \omega\} \,, \tag{6.107}$$

  which parametrize (at the level of Newtonian mechanics) the orbital motion of the pulsar. Here T_0 is a time of passage at periastron, used as a reference time, and the quantities $P_b, x = (a/c)\sin\iota, e, \omega$, which all have secular variations, are evaluated at $T = T_0$.
- The eight independently measurable post-Keplerian parameters

$$\{\dot{\omega}, \gamma, \dot{P}_b, r, s, \delta_\theta, \dot{e}, \dot{x}\} \,, \tag{6.108}$$

  which characterize the relativistic corrections to the orbital motion.

Instead, the parameters A and B which enter in the aberration formula, as well as δ_r, in practice are not separately measurable, since their effect turns out to be degenerate with that of other parameters.

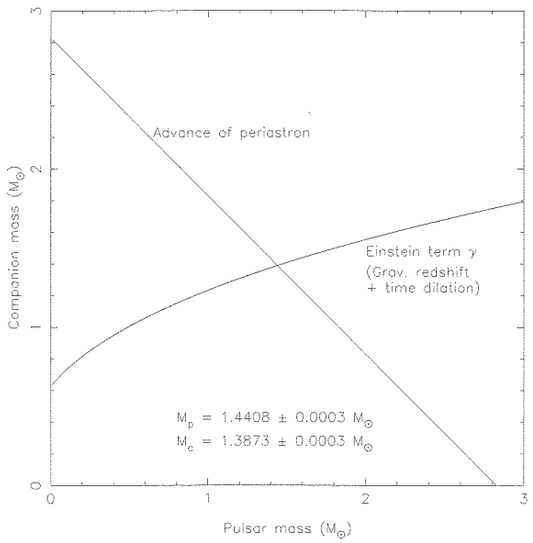

Fig. 6.6 Constraints on the pulsar and companion mass from $\langle\dot{\omega}\rangle$ and γ. The uncertainties in $\langle\dot{\omega}\rangle$ and γ are smaller than the displayed linewidths. From Weisberg and Taylor (2002). The values of the masses have been updated in Weisberg and Taylor (2004), see Table 6.1.

If we assume the validity of general relativity, all the post-Keplerian parameters are predicted once we know the value of the Keplerian parameters, and the masses of the pulsar and of the companion, m_p and m_c. Therefore, if from the fit of the observed time residuals to the timing formula we can extract the five Keplerian parameters plus any two of the post-Keplerian parameters, we can get the masses m_p and m_c. At this point, any further post-Keplerian parameter which can be extracted from the fit to the experimental data provides a test of general relativity, since it can be compared to the value predicted by general relativity, with no more free parameter at our disposal.

In particular, for the Hulse–Taylor binary pulsar it is possible to extract, from the comparison with the timing formula, all Keplerian parameters and the three post-Keplerian quantities $\langle\dot{\omega}\rangle, \gamma$ and $\dot{P}_b$. From the values of $\langle\dot{\omega}\rangle$ and γ one obtains m_p and m_c, see eq. (6.1) and Fig. 6.6. Concerning $\dot{P}_b$, the observed value is (see Table 6.1 on page 303)

$$\dot{P}_b^{\rm obs} = -2.4184(9) \times 10^{-12} \,. \tag{6.109}$$

Using the known values of the accelerations in the galactic potential, one finds $\dot{P}_b^{\rm gal} = -0.0128(50) \times 10^{-12}$. Correcting for this effect according to eq. (6.103) we therefore have

$$\dot{P}_b^{\rm intrinsic} = \dot{P}_b^{\rm obs} - \dot{P}_b^{\rm gal} = -2.4056(51) \times 10^{-12} \,. \tag{6.110}$$

Since the masses m_c and m_p have been fixed from $\langle\dot{\omega}\rangle$ and γ, the value of $\dot{P}_b^{\rm intrinsic}$ can now be compared with the prediction of general relativity

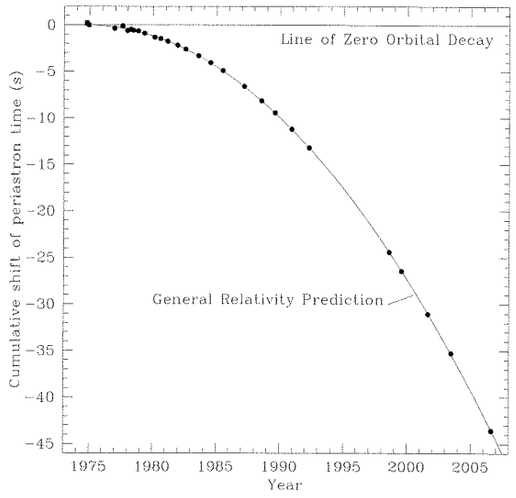

Fig. 6.7 Orbital decay of PSR B1913+16. The data points indicate the observed change in the epoch of periastron with date, while the parabola is the general relativity prediction for a system emitting gravitational radiation. From Weisberg, Taylor and Nice (in preparation). The years in the late 1990s with no data corresponds to a period when the Arecibo telescope was closed for major upgrades.

due to GW emission, eq. (6.4), which is

$$\dot{P}_b^{\rm GR} = -2.40242(2) \times 10^{-12} \,. \tag{6.111}$$

The agreement is therefore at the $(0.13 \pm 0.21)\%$ level. A vivid way to show this agreement is to plot the cumulative shift of periastron time as a function of the observation time. Similarly to what we did in eq. (6.42) for the cumulative phase of the rotation of the pulsar around its axis, we can write the accumulated orbital phase ϕ_b as

$$\frac{1}{2\pi}\,\phi_b(T) = \nu_b T + \frac{1}{2}\dot{\nu}_b T^2 + \ldots \,, \tag{6.112}$$

where $\nu_b = 1/P_b$ is the orbital frequency, and we have chosen the origin of T so that a periastron passage T_0 is at $\phi_b = 0$. For the Hulse–Taylor pulsar, the terms proportional to $\ddot{\nu}_b$ and higher are negligible. The n-th time of periastron passage, T_n, takes place when $\phi_b(T_n) = 2\pi n$, i.e.

$$\nu_b T_n + \frac{1}{2}\dot{\nu}_b T_n^2 = n \,. \tag{6.113}$$

Thus, the cumulative difference between the periastron passages T_n and the values n/ν_b is given by

$$T_n - \frac{n}{\nu_b} = -\frac{\dot{\nu}_b}{2\nu_b} T_n^2 \,, \tag{6.114}$$

or, in terms of $P_b = 1/\nu_b$,

$$T_n - P_b n = \frac{\dot{P}_b}{2P_b} T_n^2 \,. \tag{6.115}$$

This is a parabola with coefficient given by $(\dot{P}_b)/(2P_b) < 0$ and, as we see in Fig. 6.7, the agreement between the data and the theory is extremely good, and remarkably stable along the years. Observe that the uncertainty in the galactic acceleration (the first term in eq. (6.104)) dominates the experimental error, and is the limiting factor in the comparison with general relativity.

Finally, we mention that recent observations indicate a variation of the pulse profile of the Hulse–Taylor binary pulsar. This is consistent with the fact that the pulsar is undergoing geodetic precession (a general-relativistic effect due to the spin-orbit coupling). The period of this geodetic precession is about 300 yr, and the data suggest that the pulsar's beam will no longer intersect our line of sight after the year 2025, so the pulsar will become unobservable.

6.3 The double pulsar, and more compact binaries

Double NS systems are rare. Even if the original binary star system survived the first supernova explosion, it will typically be disrupted by the second supernova explosion. Furthermore, in pulsar surveys there are selection effects against NS-NS systems, because the modulation of the period of the pulsar due to its orbital motion makes the detection more difficult. Still, after the discovery of the Hulse–Taylor pulsar, PSR B1913+16, a number of other NS-NS binaries have been discovered. Presently (2007) there are five system whose identification with NS-NS binaries is considered certain, because the masses of the two stars have been measured, and found to be very close to the value $\simeq 1.3 M_\odot$ expected for a NS. These are shown in Table 6.2. Furthermore, there are at least three more binary systems (PSR J1518+4904, J1811−1736 and J1829+2456) whose identification with NS-NS binaries is very likely, although the two separate masses have not yet been measured with comparable precision. Besides, a number of white dwarf/NS binaries are known. We discuss here the most interesting systems.

The double pulsar, PSR J0737−3039

This is a very remarkable system, which is already a truly spectacular laboratory for general relativity, and will become even more so in the next few years. The pulsar PSR J0737−3039, with a period 22.8 ms, was discovered in April 2003 (Burgay *et al.* 2003), in a survey of the southern sky made with the Parkes 64-m radio telescope in Australia. It was soon found to be a member of the most relativistic binary system ever

Table 6.2 The five confirmed NS-NS binaries; τ is the time to coalescence because of GW emission, computed from eqs. (4.136) and (4.140) (setting $G(e) = 1$). For PSR J1756−2251 we assumed $m_c = 1.2 M_\odot$.

PSR	P (ms)	P_b (hr)	e	$(a/c)\sin\iota$ (s)	$m_p(M_\odot)$	$m_c(M_\odot)$	τ (Myr)
J0737−3039A	22.7	2.45	0.088	1.42	1.3381(7)		86
B	2773.6					1.2489(7)	
B1534+12	37.9	10.1	0.27	3.73	1.3332(10)	1.3452(10)	2783
J1756−2251	28.5	7.67	0.18	2.76	$2.574(3) - m_c$	< 1.25	1660
B1913+16	59.0	7.75	0.617	2.34	1.4414(2)	1.3867(2)	306
B2127+11C	30.5	8.05	0.681	2.52	1.350(40)	1.363(40)	218

discovered, with an orbital period P_b of just 2.4 hr. Thus, relativistic effects are even more important than in the Hulse–Taylor pulsar. For instance, its periastron advance is about 17 deg/yr, four times larger than for the Hulse–Taylor pulsar, and could be measured already after a few days of observations. Its coalescence time, of only about 86 Myr, is the shortest among all NS-NS systems known, see Table 6.2.[12] Furthermore, its large flux density and its narrow pulse make possible to have a high timing precision. These features would have already made this system exceptionally interesting. Then, in October 2003, even its companion was detected as a pulsar (Lyne *et al.* 2004), making it the first observed NS-NS system where both neutron stars are pulsars whose beams intersect our line of sight. The pulsar discovered first, labeled as A, is a millisecond pulsar, while the other (B) has a period of about 2.7 s (see Table 6.2). It turned out that the pulses of B change significantly along the orbital phase, probably because of the influence of the energy flux of A on its magnetosphere, so the beam from B is clearly visible only for two short periods of about 10 min each during its orbital motion (which is the reason why B was not detected initially).

The fact that we observe both beams allows us to measure separately $x_A = (1/c) a_A \sin\iota$ and $x_B = (1/c) a_B \sin\iota$, where a_A and a_B are the major semiaxes of the orbits of the A and B pulsars, respectively. Then, from Kepler's third law, we get their mass ratio,[13]

$$R \equiv \frac{m_A}{m_B} = \frac{x_B}{x_A} \,, \tag{6.116}$$

while, as usual, once the Keplerian parameters have been measured, from the periastron advance we get the total mass (see eq. (6.93)). Thus, after only two and a half years of observations, we already have a rather precise determination of the masses of the two pulsars, see Table 6.2.

Given the importance of relativistic effects in this system, it has already been possible to extract, from the fit to the timing formula, five post-Keplerian parameters, reported in Table 6.3. Observe in particular that $\sin\iota = 0.99974$, with an error $(-39, +16)$ on the last two digits, i.e.

[12] This also had the effect of increasing by almost one order of magnitude the expected coalescence rate of NS-NS systems, with very important consequences for GW detectors. We will come back to these issues in Vol. 2.

[13] It is also important to observe that eq. (6.116) is expected to hold not only in general relativity, but in any realistic theory of gravity, at least to 1PN order. Furthermore, this relation is also independent of strong-field effects, which is not the case for the post-Keplerian parameters.

the orbit is seen nearly edge-on, so it is ideally oriented for measuring the Shapiro delay. Finally, we can add to the list of virtues of this binary system that the timing results indicate that its proper motion is surprisingly small, so the proper motion corrections discussed on page 322 are small. The distance to the pulsar is estimated, from its dispersion measure, to be $d \sim 500$ pc.

Having fixed the masses using $\langle\dot{\omega}\rangle$ and the mass ratio R, we are left with four predictions from general relativity, for the four measured quantities $\dot{P}_b, \gamma, r, s$. Better yet, one can plot the six quantities $\{R, \dot{\omega}, \dot{P}_b, \gamma, r, s\}$ in the plane (m_A, m_B), and one finds that all six curves meet at one common point. As shown in Fig. 6.8, the agreement is very remarkable. In particular, for the shape of the Shapiro time delay, s, the agreement between theory and observation is

$$\frac{s^{\rm GR}}{s^{\rm obs}} = 0.99987(50) \qquad (6.117)$$

and we see that general relativity passes this test at the 0.05% level. This is by far the best available test of general relativity in strong fields, even better than the test based on the observed $\dot{P}_b$ for the Hulse–Taylor binary pulsar with a 30-year data span, compare with eq. (6.5).

Concerning the measure of $\dot{P}_b$, the precision obtained after 2.5 years of observations is given in Table 6.3. Given that the measured uncertainty in $\dot{P}_b$ decreases approximately as $T^{-2.5}$, where T is the data span, we expect that in about five years it should be measured at the level of 0.1% or better. As we mentioned, the proper motion correction to this double binary system are quite small, as well as the corrections due to differential acceleration in the galactic potential. This suggests that for this system one could eventually arrive to a measure of $\dot{P}_b$ at the level of 0.02%.

Observe that, in Fig. 6.8, only the white part of the plot is allowed, and the shaded part is excluded. This follows from the fact that, in this binary system, we can measure separately $x_A = (1/c)a_A \sin\iota$ and $x_B = (1/c)a_B \sin\iota$, where $a_{A,B}$ are the semimajor axes of the orbits of the stars A and B, respectively. From the measure of x_A, together with the orbital period P_b, one can form the *mass function*

$$f_A(m_A, m_B) = \left(\frac{2\pi}{P_b}\right)^2 x_A^3 \,. \qquad (6.118)$$

Using $a_A = (m_B/m)a$, where $m = m_A + m_B$ is the total mass, and a is the semimajor axis of the relative orbit in the CM, and making use of Kepler's law $a^3 = Gm(P_b/2\pi)^2$, the mass function can be written as

$$f_A(m_A, m_B) = \frac{G}{c^3}\frac{(m_B \sin\iota)^3}{(m_A + m_B)^2} \,. \qquad (6.119)$$

Similarly, from x_B and P_b we can form the mass function $f_B(m_A, m_B)$. Given the measured values of f_A and f_B, the condition $\sin\iota \leqslant 1$ restricts the allowed region in the (m_A, m_B) plane to the white, wedge-shaped

Table 6.3 The measured post-Keplerian parameters for PSR J0737−3039; $s = \sin\iota$ and r are the shape and range of Shapiro delay, respectively. From Kramer *et al.* (2006).

parameter	value
$\langle\dot{\omega}\rangle$ (deg/yr)	16.89947(68)
γ (ms)	0.3856(26)
$\dot{P}_b$	$-1.252(17) \times 10^{-12}$
s	0.99974(−39, +16)
r (μs)	6.21(33)

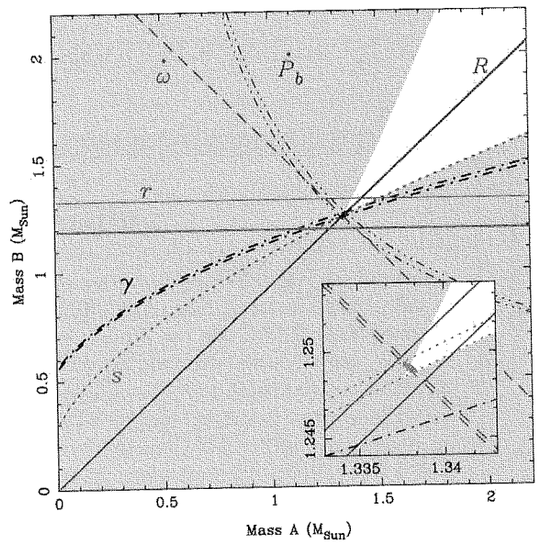

Fig. 6.8 The mass–mass diagram for the double pulsar system J0737−3039. Inset is an enlarged view of the small square where the various constraints intersect. From Kramer *et al.* (2006).

part. The fact that $\sin\iota$ turns out to be very close to one is reflected in the fact that the intersection between the various curves is very close to the cusp of the wedge-shaped region.

With more observation time, the accuracy of these data will increase further, and it is expected that one will soon have to use post-Newtonian corrections to the orbit of higher order than $(v/c)^2$. Potentially, this could allow the observation of corrections that depend on the moment of inertia of the neutron stars, and therefore to obtain a direct measure of the NS radius. This will be of great interest, since the mass–radius relation of a NS is characteristic of its equation of state, as we will discuss in Vol. 2.

PSR B1534+12

Together with the Hulse–Taylor pulsar and the double pulsar, this is the other system in which to date has been possible to measure the decrease in orbital period due to GW emission. It was discovered in 1991 with the Arecibo telescope. It is significantly brighter than the Hulse–Taylor pulsar, and its pulse has a narrow peak, allowing precise timing measurement. Furthermore, the orbit is nearly edge-on, which facilitates the measure of the range r and shape s of the Shapiro delay. As a result, after ten years of data, the five post-Keplerian $\{\dot{\omega}, \gamma, \dot{P}_b, r, s\}$ parameters have been measured. As discussed above, this in principle allows us to have three independent tests of general relativity, since these

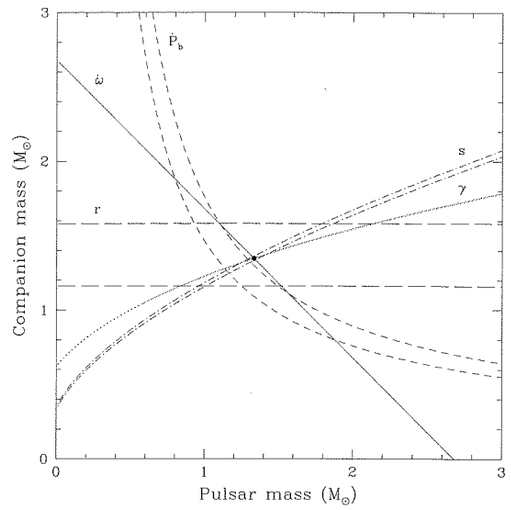

Fig. 6.9 The mass–mass diagram for PSR B1534+12. From Stairs *et al.* (2002).

five parameters are fixed in terms of the two masses m_p and m_c. We see from Fig. 6.9 that the three curves corresponding to $\dot{\omega}, \gamma$ and s meet indeed at a single point in the (m_p, m_c) plane, providing an agreement between theory and experiment at a level of about 1%. The value of r is only measured with a precision of about 20%, but still its value is centered on the general relativity prediction. There is instead a small discrepancy for $\dot{P}_b$. However, the value of $\dot{P}_b$ is quite sensitive to the correction v_T^2/d in eq. (6.104), since the pulsar has a significant proper motion and is at a close distance from us. If one estimates the distance d from the dispersion measure, one finds $d \simeq 0.7$ kpc. However, this estimate implies a model for the electron distribution in the galaxy (the quantity n_e which enters in eq. (6.37)). This model, due to Cordes and Taylor, has mostly a statistical significance, and can be in error for a single pulsar. After correcting for galactic acceleration and proper motion using eq. (6.104) with $d \simeq 0.7$ kpc, one finds

$$\dot{P}_b^{\rm obs} - \dot{P}_b^{\rm gal} = (-0.174 \pm 0.011) \times 10^{-12}\,, \tag{6.120}$$

to be compared with the prediction of general relativity

$$\dot{P}_b^{\rm GR} = -0.192 \times 10^{-12}\,, \tag{6.121}$$

so the measured value differs from this prediction by about 1.7 standard deviations. We can however reverse the logic, and assume the correctness of the prediction of general relativity for $\dot{P}_b$, which, at this level of precision, is by now established beyond any doubt from the Hulse–Taylor pulsar and from the double pulsar, and we can use the measured

value of $\dot{P}_b$ to obtain a better estimate of the distance d to the pulsar. This method yields $d = 1.02 \pm 0.05$ kpc.

Further reading

- For a general introduction to pulsars, see Lyne and Graham-Smith (2005) and Lorimer (2005). For a catalogue of pulsars see the ATNF catalogue, at www.atnf.csiro.au/research/pulsar/psrcat.
- For the discovery of PSR B1913+16, see Hulse and Taylor (1975), and the Nobel lectures of Hulse (1994) and of Taylor (1994). The observation of gravitational radiation from PSR B1913+16 is discussed in Taylor, Fowler and McCulloch (1979) and in Taylor and Weisberg (1982, 1989). An update of the results is given in Weisberg and Taylor (2002, 2004).
- Pulsar timing is reviewed in Backer and Hellings (1986) and in Stairs (2003). See also the textbooks Will (1993), Straumann (2004) and Lyne and Graham-Smith (2005). A review of the comparison with experiments of general relativistic effects such as Shapiro delay, etc. is given in Will (2006).
- An approximate timing formula was developed by Blanford and Teukolsky (1976), Epstein (1977, 1979) and Haugan (1985), and was adequate to describe the earlier data of the Hulse–Taylor pulsar, and to find evidence for GW emission, see Taylor and Weisberg (1982). With improved experimental accuracy it became necessary a full general-relativistic treatment, which was given by Damour and Deruelle (1985, 1986). Furthermore, in Damour and Deruelle (1986) it is shown how to parametrize the timing effects in a way common to a wide class of alternative theories of gravitations, performing a theory-independent analysis of the timing data, and therefore comparing general relativity to alternative theories. A comparison of different timing models is given in Taylor and Weisberg (1989). For further discussions of the full general-relativistic treatment see also Damour (1983) and Damour and Taylor (1991, 1992).
- The 1PN corrections to $\dot{P}_b$ are computed in Blanchet and Schäfer (1989). This corrections has the effect of multiplying $\dot{P}_b$ by a factor $(1 + X_{\rm 1PN})$ where, for the Hulse–Taylor binary pulsar, $X_{\rm 1PN} \simeq 2.15 \times 10^{-5}$, far below the accuracy of eq. (6.5). This correction is however larger, and potentially more important, for the double pulsar. Higher-order post-Newtonian corrections, which depend also on the moment of inertia of the star, can be important in the measurement of other relativistic parameters, such as the periastron advance, and are discussed in Damour and Schäfer (1988).
- The discovery of the pulsar PSR J0737−3039A is reported in Burgay *et al.* (2003) and the detection of the companion as a pulsar in Lyne *et al.* (2004). The resulting tests of general relativity, including orbital decay because of GW emission, are discussed in Kramer *et al.* (2005), and updated in Kramer *et al.* (2006).
- The discovery of PSR B1534+12 is reported in Wolszczan (1991), and updated measurements of its orbital decay and other post-Keplerian parameters are reported in Stairs, Thorsett, Taylor and Wolszczan (2002).